UNIVERSITAT POLITÈCNICA DE VALÈNCIA

# UNIVERSITAT POLITÈCNICA DE VALÈNCIA

## Escuela Técnica Superior de Ingeniería Industrial

# Análisis y diseño de compuestos porosos tridimensionales basados en óxido de grafeno modificado con grupos amina para almacenamiento de energía

Trabajo Fin de Máster

Máster Universitario en Ingeniería Industrial

AUTOR/A: Le Gall, Alexandre

Tutor/a: Pruna, Alina Iuliana

Cotutor/a externo: CEMBRERO CIL, JESUS

CURSO ACADÉMICO: 2023/2024

UNIVERSITAT POLITÈCNICA DE VALÈNCIA

ESCOLA TÈCNICA SUPERIOR ENGINYERIA INDUSTRIAL VALÈNCIA

UNIVERSITÉ DE LORRAINE

EEIGM
ÉCOLE EUROPÉENNE D'INGÉNIEURS EN GÉNIE DES MATÉRIAUX

# Análisis y diseño de compuestos porosos tridimensionales basados en óxido de grafeno modificado con grupos amina para almacenamiento de energía

Master's Thesis

Alexandre Le Gall

Tutor: Alina Iuliana Pruna
Co-Tutor: Jesús Cembrero

September 2023 – January 2024

UNIVERSITAT POLITÈCNICA DE VALÈNCIA

## Abstract:

Amino-modified graphene oxide aerogels are a possible solution for the future of energy storage. However, it is important to study the evolution of the properties of these materials as a function of the different amine groups that can be added and degree of functionalization. Thus, in this study, different aerogels coated with a conductive polymer, polypyrrole, by cyclic voltammetry (CV) electrodeposition. These aerogels differ in different parameters. First of all, with the presence or absence of reducing agents which aim to reduce graphene oxide such as ethylenediamine (EDA), Polyamidoamine (PAMAM) or vitamin C. But also by the fact that they have been heat treated or not, which makes it possible to improve the physical and chemical properties such as reinforcing the reduction of graphene or improving electrical conductivity. Finally, some contain carbon nanotubes (CNTs) which are tubular structures made up of graphene sheets rolled up to form a tube; they must improve the electrical conductivity of the materials.

In order to be able to analyze and compare the aerogels, a morphological characterization by SEM and FTIR as well as an electrochemical characterization by CV are carried out, enabling us to know the capacitance of each sample and to understand the difference between the values.

This study showed that, without heat treatment, an aerogel with EDA had a higher capacitance than one with PAMAN. On the contrary, with heat treatment, PAMAM outperformed EDA, although aerogels without EDA and PAMAM performed even better. Finally, this study concludes that vitamin C gives structural stability to an aerogel with heat treatment, and consequently its capacitance value is higher than for all other samples.



***Key Words: aerogel, graphene oxide, electrodeposition, polypyrrole, dendrimer***



## Resumen:

Los aerogeles de óxido de grafeno modificados con aminas son una posible solución para el futuro del almacenamiento de energía. Sin embargo, es importante estudiar la evolución de las propiedades de estos materiales en función de los diferentes grupos aminos que se pueden añadir y del grado de funcionalización. Así, en este estudio se han estudiado diferentes aerogeles recubiertos con un polímero conductor, el polipirrol, mediante electrodeposición por voltamperometría cíclica (CV). Estos aerogeles difieren en diferentes parámetros. En primer lugar, por la presencia o ausencia de agentes reductores cuyo objetivo es reducir el óxido de grafeno, como la etilendiamina (EDA), la poliamidoamina (PAMAM) o la vitamina C. Pero también por el hecho de que hayan sido tratados térmicamente o no, lo que permite mejorar las propiedades físicas y químicas, como reforzar la reducción del grafeno o mejorar la conductividad eléctrica. Por último, algunos contienen nanotubos de carbono (CNT), que son estructuras tubulares formadas por láminas de grafeno enrolladas para formar un tubo; deben mejorar la conductividad eléctrica de los materiales.

Para poder analizar y comparar los aerogeles, se lleva a cabo una caracterización morfológica por SEM y FTIR, así como una caracterización electroquímica por CV, lo que permite conocer la capacitancia de cada muestra y entender la diferencia entre los valores.

Este estudio demostró que, sin tratamiento térmico, un aerogel con EDA tenía una capacitancia mayor que uno con PAMAN. Por el contrario, con tratamiento térmico, PAMAM superó a EDA, aunque los aerogeles sin EDA y PAMAM obtuvieron resultados aún mejores. Por último, este estudio concluye que la vitamina C confiere estabilidad estructural a un aerogel con tratamiento térmico y, en consecuencia, su valor de capacitancia es superior al de todas las demás muestras.



***Palabras clave: aerogel, óxido de grafeno, electrodeposición, polipirrol, dendrímero***

Table of content

# 1 Introduction

The development of electronics in recent years has increased the demand for energy storage devices, driving the search for ever more powerful and efficient devices. This has led to the discovery of innovative materials and devices. Among these devices, supercapacitors attract attention thanks to their excellent properties.

Currently, 2 energy storage systems are in use: batteries and electrochemical capacitors. [1]
Firstly, batteries operate on reversible chemical reactions between the active materials in the electrodes and the electrolyte. During discharge, electrons are released from the electrodes, creating an electric current, while during charge, electrons are forced back to the electrodes. Batteries are classified according to the nature of their electrodes and electrolyte, such as lithium-ion, lead-acid, nickel-metal-hydride. These batteries have the advantage of offering high energy density, enabling them to store large amounts of energy, plus they are ideal for long-term energy storage due to their ability to store a significant amount of chemical energy. However, they often have longer charge/discharge times than supercapacitors. In addition, their lifespan can be affected by frequent charge/discharge cycles, and they also have the disadvantage of being heavier and bulkier, depending on their components. [2]
Secondly, electrochemical capacitors store energy in the form of ions in an electrical double layer formed at the electrode/electrolyte interface and can also include chemical reactions. They can use activated carbon as an electrode, offering a large specific surface area for ion adsorption. This energy storage solution can charge and discharge rapidly, providing high instantaneous power. What's more, they have an extended service life, particularly during frequent charging and discharging cycles. Finally, they offer high power density, making them suitable for applications requiring instant energy release. But they also have a lower energy density than batteries, which means they can't store as much energy for the same volume. They are often used for short-term energy storage, not rivalling the long-term storage capacity of batteries. Some types of electrochemical capacitors can be more expensive to manufacture. [3]

Supercapacitors thus represent a major innovation in energy storage technology. These electronic components have the exceptional ability to store and release large quantities of electrical energy quickly and efficiently. Unlike conventional batteries, supercapacitors are distinguished by their ability to deliver high power in a very short time, while offering longer life and greater stability. This exceptional performance is due to their structure and the specific composition of the materials used. The fundamental component of a supercapacitor is the electrical double layer, which forms at the interface between the electrode and the electrolyte. [4] [5]
Supercapacitor electrodes are generally made of high-surface-area materials such as activated carbon or carbon nanotubes [6]. These materials offer a large surface area, enabling the formation of an electrical double layer. In addition, supercapacitors can also use specific electrolytes, such as organic salt electrolytes or aqueous electrolytes. Ionic electrolytes enable the transport of electrical charges between electrodes, facilitating the storage and rapid release of electrical energy. In some cases, the use of graphene-based materials or specific composites helps to improve the electrical conductivity and cyclic stability of supercapacitors. [5]
Because of their outstanding performance, supercapacitors are attracting growing interest in a variety of applications, from electric vehicles to portable electronic devices. [7]

As mentioned above, carbon-based materials are often used in supercapacitors, as they offer high electrical conductivity and chemical stability [8]. However, they are not the only solution. The alternatives include three-dimensional porous composites, which appear to be a promising prospect as they combine the lightness of porous materials with the excellent properties of amine-modified graphene oxide (GO), namely high specific surface area, low density and high electrical conductivity. In

addition, highly porous materials allow electrolyte to diffuse more easily into the material [9], are mechanically stable and electrically conductive thanks to their three-dimensional network [10].

The modification of graphene oxides with amines aims to improve the performance of these energy storage devices. Graphene oxides, often used due to their abundance and promising electrochemical properties, benefit from amine modification to optimize their electrical conductivity, increase their storage capacity, and promote rapid electrochemical responses.
The introduction of amine groups, such as aliphatic amines like ethylenediamine (EDA) or aromatic amines like aniline, onto the surface of graphene oxides can improve electronic conductivity by facilitating the transport of electrical charges through the material. In addition, the modification can influence the porous structure of graphene oxide, thereby increasing the specific surface area available for ion adsorption. This increase in specific surface area contributes to the supercapacitor's energy storage capacity. In addition, interactions between modified amine groups and the electrolyte used can improve the cyclic stability of the device. Amines can also play a role in reducing overvoltage phenomena and regulating the interfacial properties between electrode and electrolyte. [11] [12] [13]
A specific example could be the use of amines such as ethylenediamine (EDA) to modify graphene oxides, where functionalization can lead to a significant improvement in supercapacitor performance in terms of power density, specific capacitance, and long-term stability.

However, despite its favorable properties, this solution has insufficient specific capacitance to store electrical charges, even though this has already been greatly increased by the modification brought about by the amine groups [8]. So, with the aim of increasing this specific capacity, other pseudocapacitive materials are being used to fabricate composite aerogels with improved electrochemical performance [14]. These include conductive polymers, which offer a unique combination of lightness, flexibility and electrical conductivity.

These polymers, such as polypyrrole (Ppy), polyaniline (PANI) and polythiophene (PTh), can be integrated into the aerogel structure to exploit their intrinsic conductivity properties. During aerogel manufacture, conductive polymers are typically deposited on the three-dimensional aerogel matrix, creating a conductive network within the porous structure. This modification improves the aerogel's electrical conductivity, facilitating the rapid transport of electrical charges. In addition to improving conductivity, these polymers can also help increase energy storage capacity by providing additional active sites for electrolyte ion adsorption. What's more, the flexibility of conductive polymers means that aerogels can adopt a variety of shapes, adapting to different electronic device configurations. Finally, they can undergo rapid, reversible electrochemical reactions without structural degradation. [15] [16]

One such polymer is polypyrrole (Ppy), which thanks to its properties such as high electrical conductivity, high electrical activity, pseudocapacitive properties, simple preparation, low preparation costs and appreciable thermal stability make it an excellent candidate for the synthesis of supercapacitors [17]. Moreover, it is interesting to add that this conductive polymer has a higher conductivity than carbon, but a lower specific surface area, which is why it is most often deposited on a porous material, as in our case with graphene aerogels, to further improve specific capacitance properties [18].

There are many polypyrrole (Ppy) composites used in supercapacitors, offering a diverse range of specific properties, depending on the materials with which they are combined.
Firstly, Ppy/carbon composites, whether activated carbon or carbon nanotubes, benefit from the synergistic combination of Ppy and carbon, exploiting carbon's large specific surface area to increase energy storage capacity while maintaining high electrical conductivity. [19]

Secondly, Ppy/metal oxide composites, such as Ppy/$MnO_2$ or Ppy/$RuO_2$, take advantage of the properties of metal oxides to enhance electrochemical reactivity, thus contributing to an increase in supercapacitor capacity and efficiency. [20]
In addition, Ppy/conductive polymer composites, such as Ppy/PANI or Ppy/PTh, capitalize on the synergy of the two polymers' electrical conductivity properties, offering significant advantages in terms of overall electrochemical performance, cyclic stability and reactivity. These specific properties make Ppy composites a versatile category in supercapacitor development, providing customized solutions to meet the specific needs of energy applications ranging from portable devices to larger energy storage systems. [21] [22]
Finally, Ppy/graphene oxide (GO) composites capitalize on graphene's exceptional properties, such as high conductivity and large specific surface area, to significantly enhance electrochemical reactivity and increase supercapacitor capacity. [23]

It should also be noted that polypyrrole has a higher conductivity than carbon, but a lower specific surface area, which is why it is most often deposited on a porous material, as in our case with graphene oxides. As a result, the latter set of materials enables us to improve and obtain better specific capacitance values, as shown in Table 1, compared with the other composites in the list.

| Ppy composites | Csp (F/g) |
|---|---|
| Ppy/carbon | 159 |
| Ppy/$MnO_2$ | 205 |
| Ppy/PANI | 209 |
| Ppy/GO | 233 |

*Table 1: Specific capacitance value for different Ppy composites [19] [20] [21] [23]*

Although various methods exist for depositing polypyrrole, one of the simplest, is electrodeposition, including varying deposition modes such as cyclic voltametric cycle (VC), and galvanostatic and potentiostatic depositions. The CV method is the most employed one as it is simple, fast and allows a controlled deposition beside being a relatively inexpensive method as compared with other ones such as CVD (Chemical Vapour Deposition) [24]. What's more, it's well suited to the deposition of small, complex shapes such as aerogels [25].

As a reminder, aerogels are porous materials, and it's this porosity that improves electrochemical performance and therefore its specific capacitance, beside the reduction degree and stacking of the sheets, in case of graphene based aerogels. Such characteristic can be tailored by adding various reducing agents, CNT dendrimer or heat treatments, thus, to further improve its properties [10].

The aim of this study is to investigate the evolution of the specific capacitance of different aerogels modified with amine groups such as EDA, PAMAM or vitamin C, but also with CNT added or exposed to heat treatment. All these aerogels have undergone the same CV electrodeposition of Ppy. It will therefore be possible to compare them by carrying out morphological as well as electrochemical characterization in order to find the most efficient solution for energy storage.

# 2 Materials and Methods

## 2.1 Materials

Aqueous GO slurry (monolayer content > 95%) was supplied by Graphenea (Donostia, Spain), CNTs (NC7000 series, multiwall, average diameter 9.5 nm, average length 1.5 μm) were supplied by Nanocyl (Sambreville, Belgium), Polyvinylpyrrolidone (PVP–K90, molecular biology grade) was supplied by Scharlab (Barcelona, Spain), G7 (PAMAM dendrimer) (ethylenediamine core, generation 3.0, solution 20 wt.% in methanol) was sup- plied by Sigma-Aldrich (Madrid, Spain). The rest of the reagents were supplied by Alfa Aesar (Madrid, Spain). The electrolytes were obtained with distilled water.

The various sets and samples of graphene oxide aerogels (GO) were prepared prior to the experiments carried out in this thesis. All were synthesized by a hydrothermal process with a homogeneous aqueous dispersion of GO at 2mg/mL. This was common to all samples, and in some cases no reducing agent was added. In cases where reducing agents were added, there were 3. Firstly, ethylenediamine (EDA) in a GO:EDA mass ratio of 1:2.5. Secondly, PAMAM (generation 7, G7) in a GO:G7 mass ratio of 1:0.1. The last reducing agent employed is Vitamin C (vitC) in a GO:vitC mass ratio of 1:2.5.

All these dispersions, with or without reducing agent, were then sealed and maintained at 140°C for 4h in an oven. The hydrogels obtained were then freeze-cast in liquid nitrogen ($N_2$) (at around -200°C). Lyophilization with a Lyomi Cron freeze dryer (Coolvacuum Technologies, Barcelona, Spain) was further applied for 3 days to obtain the corresponding aerogels.
Some aerogels then underwent heat treatment (TT), at 800°C for 1h in nitrogen gas ($N_2$) in order to study the effect of induced reduction of GO onto the capacitance values.

The obtained samples were divided into 3 different sets depending on the precursor GO, reducing agents and annealing treatment conditions that were used.

First of all set A, were obtained from two types of GO, one is exfoliated, and the other is not (GOx and GO). Here, the reducing agent used is EDA for both cases.
This set is made up of 5 different samples which are as follows:

- GO(TT) : GO no exfoliated, without EDA and with thermal treatment
- GOEDA : GO no exfoliated, with 2,5 EDA and without thermal treatment
- GOEDA(TT) : GO no exfoliated, with 2,5 EDA and with thermal treatment
- GOxEDA : GO exfoliated, with 2,5 EDA and without thermal treatment
- GOxEDA(TT) : GO exfoliated, with 2,5 EDA and with thermal treatment

Then set B, the reducing agent used here is dendrimer G7, having larger amount of amine groups to functionalize the GO sheets within the aerogel and therefore the ratio was reduced to 0.1 with respect to EDA samples. It should also be noted that all GO are exfoliated (GOx) in this set. Additionally, a 3 mg/mL ethanolic dispersion of carbon nanotubes (CNT) was obtained by adding CNT to ethanol together with polyvinylpyrrolidone (PVP) as a dispersing agent in a 1.5:1 CNT:PVP w/w ratio followed by ultrasound treatment for 1h. The CNT dispersion was added in a small concentration as 50 μg/mL to the dispersion of GO to further separate the GO sheets by ultrasound treatment and thus, improve the later functionalization with the PAMAM molecules by hydrothermal synthesis.

The 3 samples in this set were labeled:

- GOxCNT(TT) : GO exfoliated, with CNT, without 0,1 G7 and with thermal treatment
- GOxCNTG7(TT) : GO exfoliated, with CNT, with 0,1 G7 and with thermal treatment
- GOxCNTG7 : GO exfoliated, with CNT, with 0,1 G7 and without thermal treatment

Finally the last set, set C. This is the only set without dendrimer because its reducing agent is Vitamin C (vitC). In the latter case the graphene oxide is either exfoliated or not (GOx and GO).
The samples were named as follows:

- GOvitC(TT) : GO no exfoliated, with 2,5 Vitamin C and with thermal treatment.
- GOxvitC(TT) : GO exfoliated, with 2,5 Vitamin C and with thermal treatment

## 2.2 Preparation of the working electrode

The working electrodes were prepared from the aerogels previously prepared and cited above. To do this, the aerogels are cut into thin slices and then these slices are cut into a square or rectangle, seeking to have a surface area of more or less 20 $mm^2$.
Further, the slices samples were subjected to hot pressing under 1 tons and 100°C. They were placed between 2 metal plates which made it possible to directly have thin slices aerogels.

The different cut samples are then measured in three dimensions with a caliper and weighed with a precision balance in order to have maximum information to be able to compare them and carry out various calculations afterwards.

The working electrode is then prepared by attaching a piece of aerogel to a conductive glass plate, a plate which has previously been cleaned by several ultrasonic bath cycles in soapy water and distilled water. The aerogel is thus brought into contact with the conductive surface of the plate and is then taped, allowing space for contacting the electrode at one edge. Additionally, the surface areas of aerogel in contact with the electrolyte were measured with a caliper, and the active mass of aerogel was obtained.
Finally, the aerogel, glass plate and adhesive tape assembly is then weighed on a precision balance to subsequently determine the mass of polypyrrole deposited by subtracting the other components.

## 2.3 Electrodeposition of conducting polymer

Electrodepositions were carried out in a three-electrode configuration connected to an Autolab/PGSTAT101 Metrohm potentiostat. The three electrode types are the electrodes mentioned above as the working electrode, a Pt wire as the counter electrode, and an Ag/AgCl electrode as a reference electrode. The electrolyte is an aqueous solution of 0.5 M KCl and 0.1 M pyrrole.

Once all the electrodes are ready, they are immersed in the electrolyte a few minutes before the start of electrodeposition so that the aerogel is impregnated by the solution.

Electrodeposition is carried out by cyclic voltammetry (CV) on all samples, with a potential ranging from 0 to 1 V at a scan rate of 50 mV/s for 10 cycles. After deposition, the samples are rinsed with distilled water.

## 2.4 Characterization

### 2.4.1 SEM

Morphological analysis was studied by using a Gemini scanning electron microscope (SEM) connected to an energy-dispersive analyzer (Zeiss Microscopy, Oberkoche, Germany, 1.50kV).


*Figure 1: Photo of a Gemini scanning electron microscope (SEM)*

SEM is a powerful characterization technique used to examine the surface of samples at nanometric scales. This method produces high-resolution images that provide morphological and topographical details of the material under analysis. These images can reveal information on size, shape, surface roughness and other characteristics.

To achieve this, the SEM relies on the principle of electron-matter interaction by scanning a sample with a high-energy electron beam across its surface. When the electrons interact with the sample, various signals are generated, the most common of which are backscattered electrons (BS) and secondary electrons (SE). These signals are collected and used to form an image of the sample surface.

Secondary electrons are particularly important for obtaining high-resolution images, as they are emitted from the surface layer of the sample. When they strike the sample, they can give up some of their energy to one of the electrons in the sample's atoms, thus ejecting it. These electrons have a low energy because they are emitted by layers close to the sample surface. This makes it possible to detect a large number of them and obtain a high-resolution image, as well as information on the topography of the material's surface.

Backscattered electrons result from the interaction of electrons in the beam with the nuclei of atoms in the sample. These are then re-emitted in a direction close to that of the beam, with little loss of energy. Unlike secondary electrons, backscattered electrons have a high energy and will therefore produce images with lower resolution. What's more, they react differently depending on the atom: if the atom has a high atomic number, it will re-emit more electrons, and these areas will appear brighter

on the image. This information can give us a qualitative estimate of the chemical composition of the sample under study. [26] [27]

### 2.4.2 FTIR

Fourier transform infrared spectroscopy (FTIR) was studied by using an FT/IR-6200 (Jasco, Madrid, Spain) spectrometer in the ATR mode.


*Figure 2: Photo of an FT/IR-6200*

FTIR is a powerful analytical technique based on the fact that molecules absorb energy in the infrared region of the electromagnetic spectrum. This means that molecules are capable of vibrating at specific frequencies, and these vibrations absorb infrared photons corresponding to these frequencies. Infrared spectroscopy measures this absorption and provides information on molecular bonds, functional groups and the chemical structure of a compound.

This method uses an infrared light source which is directed through a Fourier interferometer. This interferometer divides the infrared beam into two parts, passes them through a sample and a reference, and then recombines them. By modifying the optical path difference between the two beams, an interferogram is obtained. Using the Fourier transform of this interferogram, we can then obtain the infrared spectrum of the compound under study.

Once the spectrum is obtained, which is graphed with absorbance (or transmittance) as a function of wavenumber (inverse of wavelength), the spectrum shows peaks at characteristic positions, which are associated with the vibrations of molecular bonds. These vibrations are of various types: bending, twisting and stretching of the bonds between atoms. These peaks can therefore be used to identify the functional groups present in the compound, giving an idea of the composition of the sample and the bonds present between atoms. [28] [29]

## 2.5 Electrochemical measurements

The electrochemical measurements of the different samples are studied by cyclic voltammetry (CV) using the same equipment as to carry out the electrodeposition, that is to say, an Autolab/PGSTAT101 Metrohm potentiostat and a three-electrode configuration.

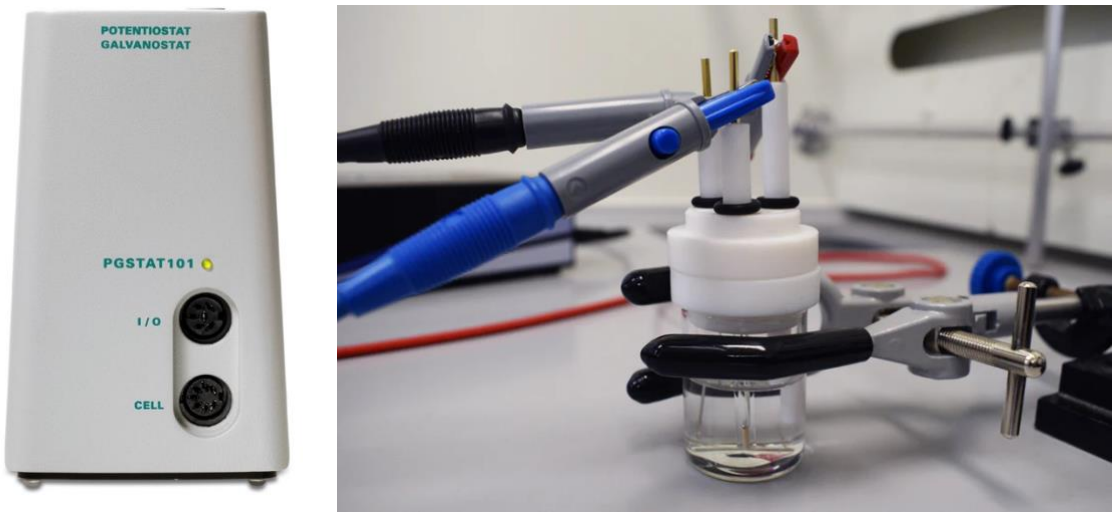


*Figure 3: Photo of an Autolab/PGSTAT101 Metrohm potentiostat and a three-electrode configuration*

These are set up in 3-electrodes system with the same electrodes, the aerogels as the working electrode, a Pt wire as the counter electrode and Ag/AgCl as the reference electrode. The electrolyte is now an aqueous solution containing 0.5M $Na_2SO_4$.

The measurements are carried out with a potential ranging from -0.2 to 1 V. Different scanning speeds are studied with 100, 50, 25, 10, 5 and 1 mV/s for the duration of one cycle.

Once all measurements have been made, the results are collected and analyzed with Origin software. The absolute area of the curve is then calculated using the software, which will make it possible to determine the polypyrrole deposition load on the aerogel.
In addition, the samples, after having been rinsed with distilled water and then dried, are weighed using a precision balance. Thus, by calculating the difference in mass between before and after electrodeposition, it is possible to know the mass of aerogel and polypyrrole that was exposed during the electrochemical measurements, and therefore to calculate the specific capacitance of each sample, but also to know the quantity of polypyrrole deposited on the aerogel.

The formulas used to calculate the specific deposition charge and capacitance are:

For deposition Charge:

$$Q(C) = \frac{A \times A_{active}}{\nu} \quad (1)$$

For specific capacitance:

$$Csp(F/g) = \frac{A \times A_{active}}{\nu \times m_{active} \times \Delta V} \quad (2)$$

Where A is the absolute area of the integration (AV/cm$^2$), $\nu$ is the scan rate (mV/s), $\Delta$V is the potential window (V), $A_{active}$ is the area exposed (cm$^2$) and $m_{active}$ is the mass exposed (g).

# 3 Results

## 3.1 Morphology

### 3.1.1 SEM characterization of aerogels prior to Ppy deposition

Analyzing SEM images is a very practical method for observing the different morphologies of aerogels with or without polypyrrole deposition.

The first thing that can be noticed with these different images of different types of aerogels is that the aerogels have a highly porous and interconnected 3D network. GO sheets can be seen randomly oriented and with the presence of some contrast between them, indicating a stacking of several layers. These images give the impression that the surface of the aerogels is relatively smooth, making them a suitable substrate for Ppy electrodeposition [8]. In addition, the large number of pores will facilitate the impregnation of the electrolyte into the substrate and thus promote better distribution of the Ppy during electrodeposition.

If we first take a closer look at figure 4a,b, we can see that the GO aerogel without heat treatment or electroplating exhibits everything we said earlier, a rather inhomogeneous distribution of pores with irregular dimensions, a randomly oriented stacking of sheets, a rather smooth surface.

Figure 4c shows the morphological evolution with the addition of a dendrimer. Indeed, the G7-modified aerogel shows an improved distribution with smaller pores, and the GO sheets appear to show less stacking given their increased transparency. Thus, reducing pore size while having a larger number of pores provides a larger active surface and therefore improves Ppy deposition.

The GOxCNT(TT) aerogel in figure 4f i.e. the one with CNTs only, appears more porous than the conventional GO. This could be explained by the presence of CNTs, which are also used as spacers. In other words, they prevent the graphene layers from re-stacking and agglomerating, which in turn improves the aerogel's porosity.

Finally, figure 4g,h shows an aerogel with dendrimer, G7, and CNT prior to electrodeposition. Thanks to a higher magnification of the image, the incorporation of CNTs between the visible GO sheets, indicated by the arrows, is more clearly visible. In addition, these enlargements confirm what was said for figure 4c, as no large pores can be distinguished, confirming the decrease in their sizes, but it is also more difficult to notice the contrast between the sheets due to greater transparency.
In addition, these images suggest that the CNTs are several microns long. [30] [31]

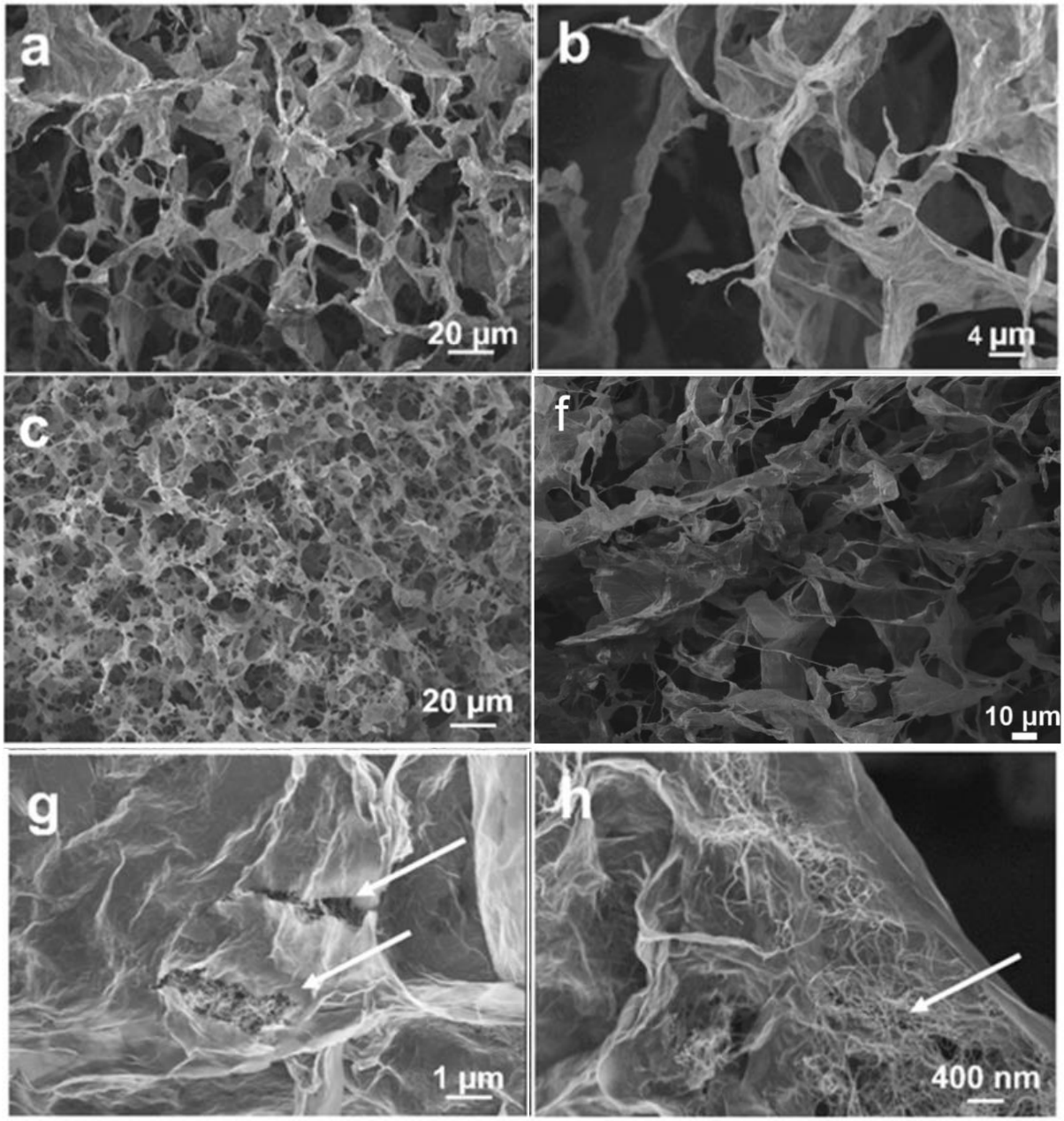


*Figure 4: SEM images of aerogels before coating with Ppy (a and b) GO, (c) GOG7, (f) GOxCNT(TT), (g and h) GOxCNTG7*

### 3.1.2 SEM characterization of aerogels after Ppy deposition

It is also interesting to compare the images obtained for an aerogel after Ppy electrodeposition. The following figure shows the classic GO aerogel as above after electrodeposition, showing a morphology typical of electrodeposited Ppy. Indeed, the surface is rougher but also covered with more or less spherical particles. What's more, the pores got covered, even though the aerogel surface is in relief, and it is no longer possible to see between the different layers. To complete the picture, these polypyrrole particles form a homogeneous, continuous network with a globular microstructure over the entire aerogel surface, proving that electroplating has been successful. [30] [31]

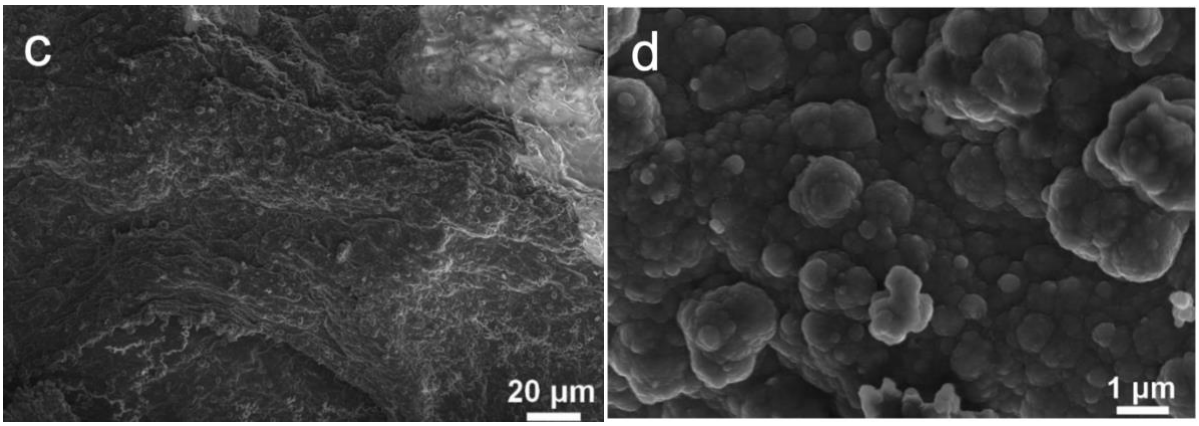


*Figure 5: SEM images of (c and d) aerogel coated with Ppy*

### 3.1.3 FTIR

Both the reduction of GO sheets in the dispersion by hydrothermal technique to obtain aerogel and the modification with amine groups could be achieved by FTIR analysis. The FTIR analysis shown in figure 6 enables us to analyze and observe the modification of typical GO spectra when reducing agents, in this case G7 (PAMAM), are incorporated. This technique enables us to understand the evolution of the amine dendrimer groups present in aerogels, as the spectra show for varying amount of amine modifier. The black line of GO corresponds to GO dispersion, the green line denoted with 0 represents the reduction of the GO as aerogel was analyzed, i.e. without the presence of a reducing agent. And finally, the red line denoted with 0.2 (the concentration of 0,2mg/mL) which corresponds to GOG7.

Taking a closer look at the figure below, GO aerogel shows typical FTIR bands located at 1614 $cm^{-1}$ attributed to C=C stretching in the aromatic rings and a broad band centered at 3000 $cm^{-1}$ attributed to C-OH due to intercalated water molecules.
GO aerogels have various functional groups: carboxyl COOH at 742 $cm^{-1}$, ketones C=0 at 884 $cm^{-1}$, C-O at 1049 $cm^{-1}$, C-O-C at 1218 $cm^{-1}$, OH and C=O at 1424 $cm^{-1}$, C=O at 1584 $cm^{-1}$ and COOH at 1714 $cm^{-1}$. [32]

When the GO aerogel is exfoliated, changes occur on the green curve. The spectra show fewer intercalated water molecules, while two bands at 742 and 884 $cm^{-1}$ disappear, the band at 1424 $cm^{-1}$ decreases in intensity and the band at 1714 $cm^{-1}$ becomes more intense. These differences in the FTIR bands show the elimination and conversion of oxygen functional groups in the GO aerogel during its reduction.

Then, by the addition of the dendrimer to the sample, new amide peaks appear at 1549, 1452, 1225 and 1086 $cm^{-1}$, corresponding to the coupling of the C-N stretching vibration. A further vibrational

band at 1630 $cm^{-1}$ attributed to the C=O amide stretching vibration mode corresponding to $NH_2$ deformation also appears. The appearance of these new bands confirms the presence of amine modification of the aerogel, by cross-linking between the carboxylic groups of GOs and the amine groups of modifiers, whether it is dendrimer G7 or EDA. [32]

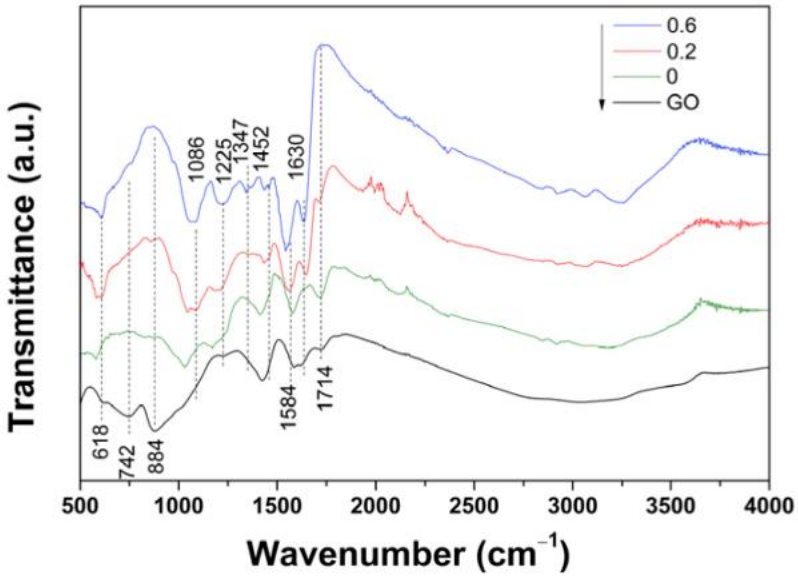


*Figure 6: FTIR spectra of GO dispersion, GO aerogel non modified and modified with amine in increasing concentration (mg/mL)*

## 3.2 Electrodeposition of polymer

First of all, before studying and determining the capacitance value Csp for each sample, it is interesting to observe and analyze a cyclic voltammogram of Ppy electrodeposition.
Figure 7 below shows an example of CV electrodeposition on GO(TT). Three different cycles are represented on the graph: the first, the fifth and the tenth cycle, in order to compare the evolution of the deposit from start to finish.
The first cycle is different from the other two. Indeed, this first cycle has a much weaker peak and reaches a much lower current density value. This can be explained by the fact that it's the start of the reaction, and so the pyrrole is beginning to oxidize, making it more conductive and thus increasing the current. We can see that the fifth and tenth cycles have a much more pronounced peak with a higher current density value. This means that the reactions are taking place more rapidly, as the current continues to increase with each cycle, and therefore the deposition of Ppy on the aerogel is greater after each cycle, without reducing the current density.

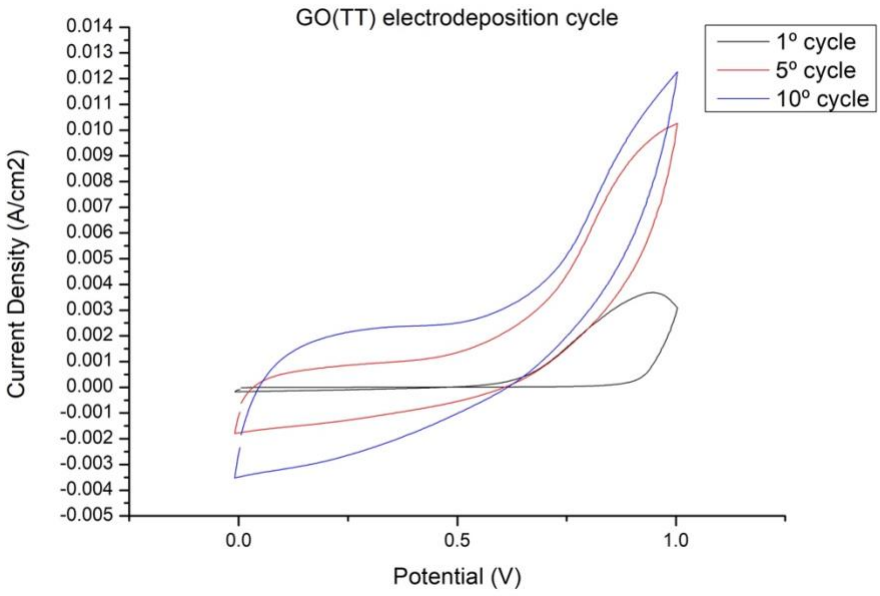


*Figure 7: Electrodeposition of Ppy on GO(TT) by CV*

It should be noted that for all the samples studied below, the electrodeposition graphs were similar, with an increase in the current density value for the tenth cycle and a more pronounced peak.

## 3.3 Capacitance measurement by cyclic voltammetry

### 3.3.1 Effect of different amine groups

Now that the Ppy electrodepositions have been carried out on the different samples, it's interesting to compare the different CV curves obtained at 10 mV/s as well as the Csp values to determine which aerogels are the most efficient and with the best capacitance.

First, the comparison begins with samples that have not been thermal treated. Below are the curves and values for GOEDA and GOxEDA, i.e. the aerogels in set A with EDA as the reducing agent.

What we notice is that the sample that has been exfoliated, i.e. GOxEDA, has a higher capacitance. This could mean that, without thermal treatment and for the same reducing agent, an exfoliated graphene oxide that has undergone Ppy electrodeposition can store more energy. This can be explained by the fact that for the 2 samples, the amount of Ppy deposited is almost identical. However, in the case of GOxEDA, exfoliation results in a greater presence of pores, thereby increasing its active surface area. With a larger active surface area than GOEDA, its ability to store energy is greater, resulting in a higher capacitance.

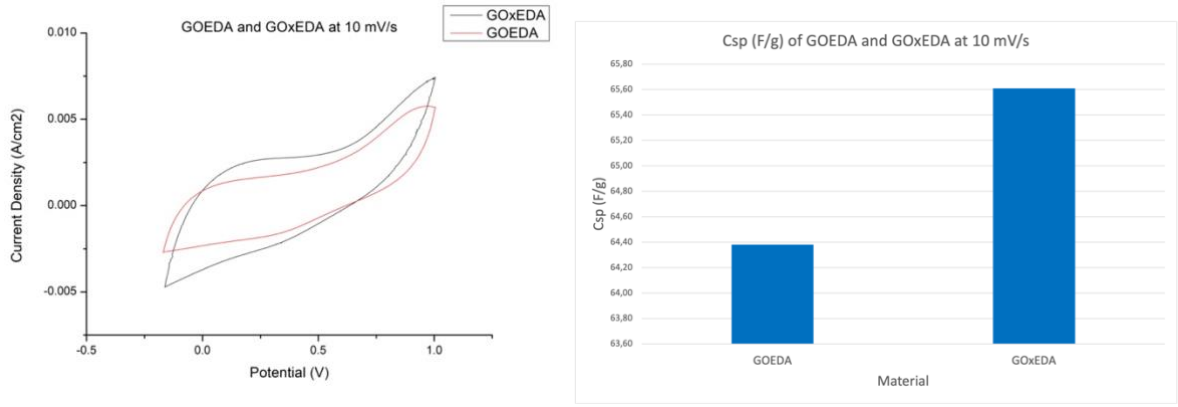


*Figure 8: CV curves and Csp values for GOEDA and GOxEDA*

To continue the comparison of aerogels that have not undergone thermal treatment, GOxCNTG7 from set B can be added. As can be seen, its Csp is lower, and its CV curve has a lower peak than the other two. So, although GOxCNTG7 has a higher exfoliation, which might lead us to believe that its active area would be higher, when the reducing agent is used, the opposite is true. This can be explained by the shape of the G7 (PAMAM), which is generally spherical and characterized by an internal molecular architecture of tree-like branches [33]. The EDA, on the other hand, has a more linear shape. This difference in shape between the reducing agents means that EDA distributes better, whereas G7 forms non-homogeneous links in the aerogel and upon deposition of Ppy, it impedes the diffusion of the ions from the electrolyte. This reduces its capacitance as compared with GOEDA and GOxEDA.

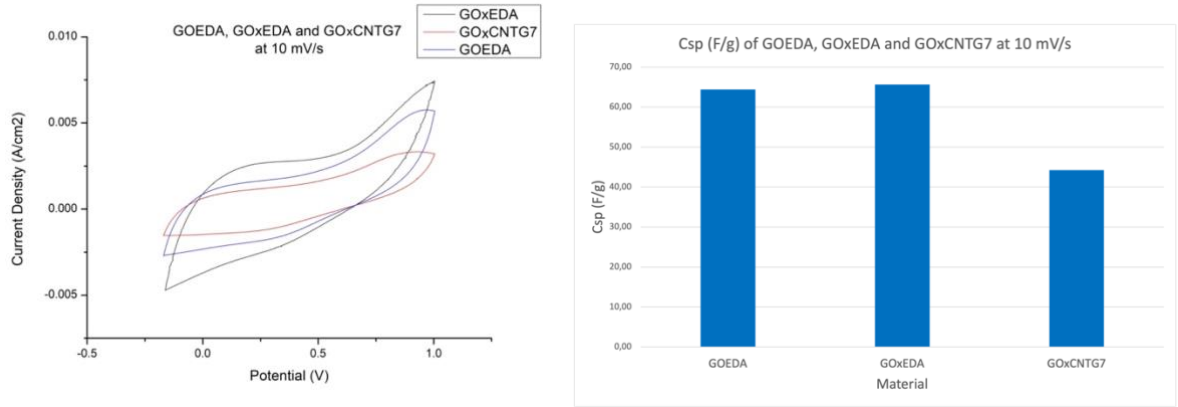


*Figure 9: CV curves and Csp values for GOEDA, GOxEDA and GOxCNTG7*

### 3.3.2 Effect of thermal treatment

First, let's take a look at the samples from set A, shown in figure 10. The first thing we notice is that the less oxidized, reducing agent-free aerogel, GO(TT), has a higher Csp value and rather showing a behavior closer to a battery than supercapacitor, given the obvious peaks in the CV. The GOEDA(TT) and GOxEDA(TT) show a more supercapacitor like behavior as the CV is rather rectangular, for the most part of the potential window. This can be explained by the fact that thermal treatment has compressed and stuck the aerogel pores by stacking. This effect is greater in the presence of reducing agents such as EDA, as the stacking upon thermal treatment is at greater extent, reducing access to the various pores and thus reducing its capacity to store energy.

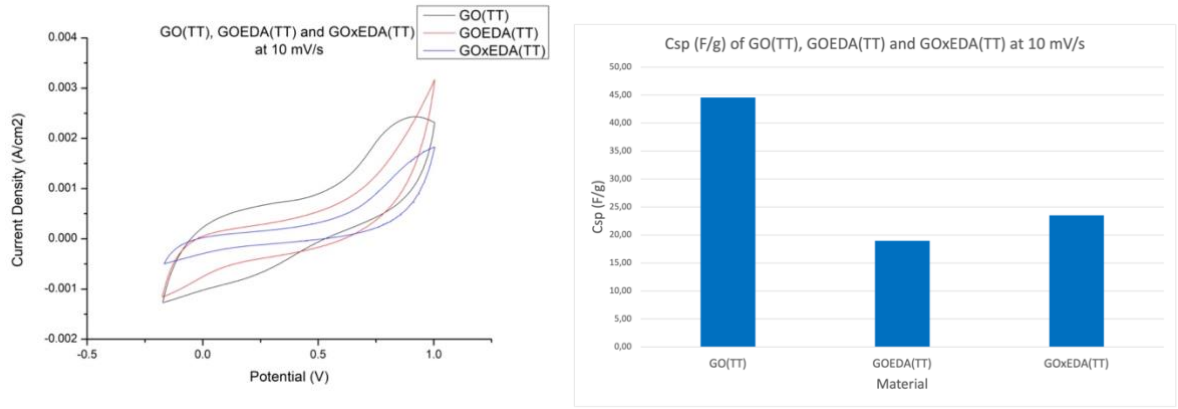


*Figure 10: CV curves and Csp values for GO(TT), GOEDA(TT) and GOxEDA(TT)*

Turning now to set B, which has dendrimer G7 as its reducing agent, we see the same thing as before. The aerogel with no reducing agent has a higher gravimetric Csp value which could be attributed to the aerogel being less conductive, so the Ppy deposition is achieved at less extent, specifically in lower thickness, thus, leaving a larger active surface area and consequently a higher capacitance. In presence of amine groups from the G7 dendrimer, the problem of thermal treatment remains, as the aerogels are once again stuck, cancelling out the effect of the reducing agents.

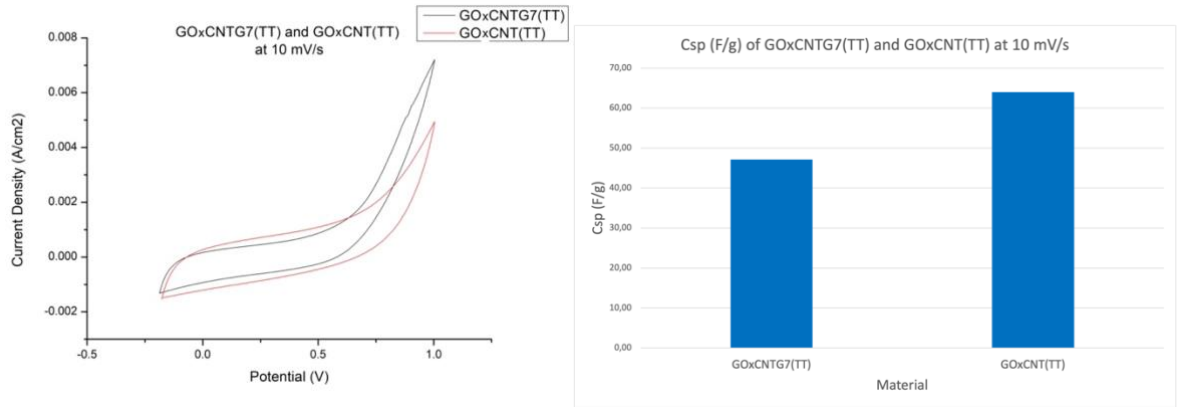


*Figure 11: CV curves and Csp values for GOxCNTG7(TT) and GOxCNTG7 (TT)*

As a reminder, in the case of non-annealed samples, the presence of EDA resulted in better Csp values than the use of G7. In the case of thermal-treated aerogels, however, the opposite is true. In fact, GOxCNTG7(TT) has a higher Csp value. As before, this is due to the geometric shape of the reducing agents, but unlike in the previous case, here the samples are stuck, and the circular shape of the G7 as well as the presence of CNT help to limit this negative effect. Thus, by being less stuck, it will be further doped, giving it a better capacitance than aerogels composed of EDA.

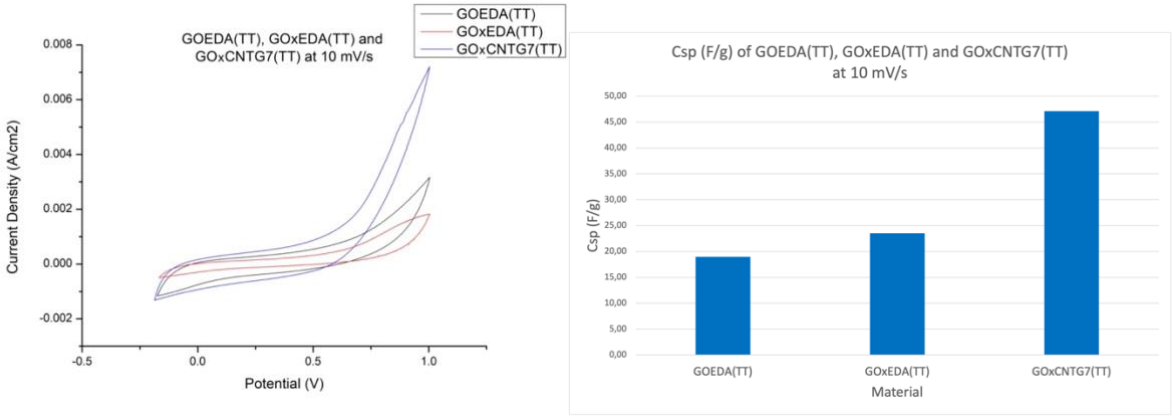


*Figure 12: CV curves and Csp values for GOEDA(TT), GOxEDA(TT) and GOxCNTG7(TT)*

Figure 13 below shows whether an aerogel based on oxidized GO, without the presence of a reducing agent outperforms classic graphene oxide. The CV curves show a stronger and larger peak for GOxCNT(TT), as do the Csp values, which are higher for the latter. So, even with heat treatment, an aerogel with more pores obtained by combining more oxidized GO and content of CNT will be less stuck and therefore have a larger active surface and consequently better capacitance.

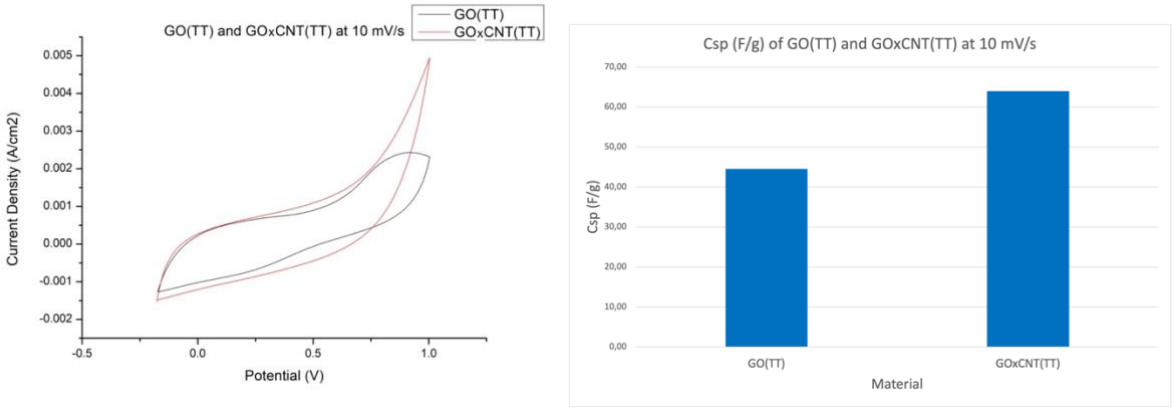


*Figure 13: CV curves and Csp values for GO(TT) and GOxCNT(TT)*

Continuing with the study of thermal treated samples, it's time to turn our attention to set C aerogels, i.e. those with vitamin C as the reducing agent.
To begin with, it's interesting to compare non-exfoliated graphene oxide. The comparison is between GOEDA(TT) and GOvitC(TT), whose curves and values are shown in figure 14. Looking at the CV curves, we notice that the curve for GOvitC(TT) is much fuller and with a more pronounced peak than that for GOEDA(TT). This difference is confirmed by looking at the Csp values, where GOvitC(TT) has a much higher capacitance. At first sight, this shows that vitamin C appears to be a much more effective reducing agent than EDA.

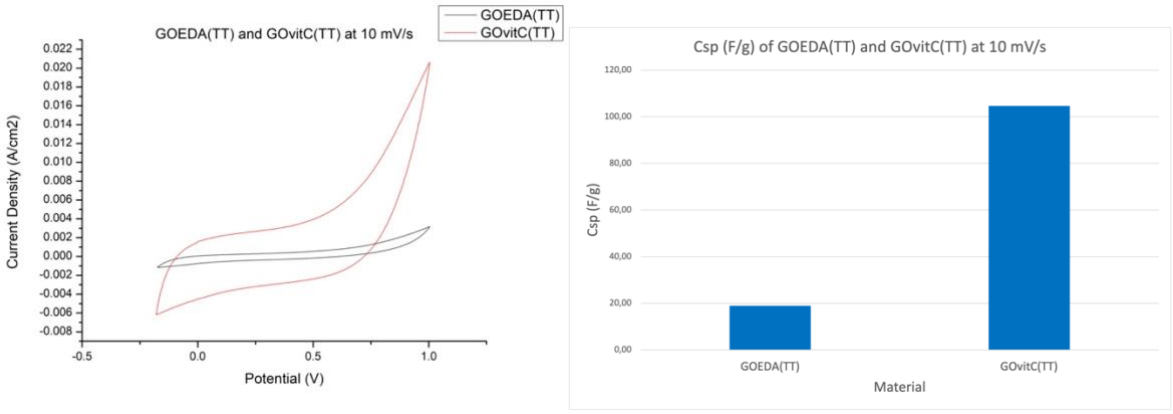


*Figure 14: CV curves and Csp values for GOEDA(TT) and GOvitC(TT)*

To complete the above comparison, we need to look at the case where the GO in the aerogel is exfoliated. As can be seen in figure 15 below, the CV curve for the sample containing vitamin C is greater, as is the Csp. Even if we take into account the Csp value for GOxCNTG7(TT), which is 47 F/g, this aerogel performs much less well. This shows that vitamin C seems to be a much more effective reducing agent than the others. This could be explained by the fact that, with thermal treatment, the other aerogels are stuck, which is not the case with the two vitamin C samples. This would mean that the vitamin C gives the aerogel structural stability, enabling it to retain a much larger active surface, hence the higher capacitance.

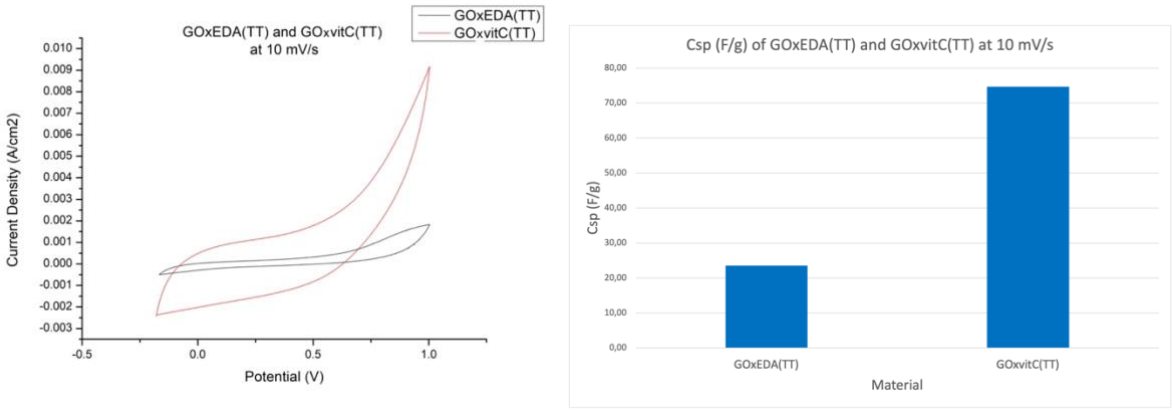


*Figure 15: CV curves and Csp values for GOxEDA(TT) and GOxvitC(TT)*

So, to finish comparing all the samples, it's interesting to analyze the results for the two aerogels in set C. What we notice is that the CV curve for GOvitC(TT) is larger and has a stronger peak, which is confirmed by the Csp value, which is much better for the latter. This would mean that in the case of an aerogel using vitamin C as a reducing agent, exfoliated graphene would be less efficient for energy storage. This could be explained by the fact that greater oxidation makes the aerogel more porous, leading to tapping the pores upon the Ppy deposition, which in turn reduces the active surface area and hence capacitance. And all this takes place thanks to the stability provided by vitamin C, which allows better access to all the aerogel's pores than in the other samples, resulting in greater Ppy deposition and lower capacitance.

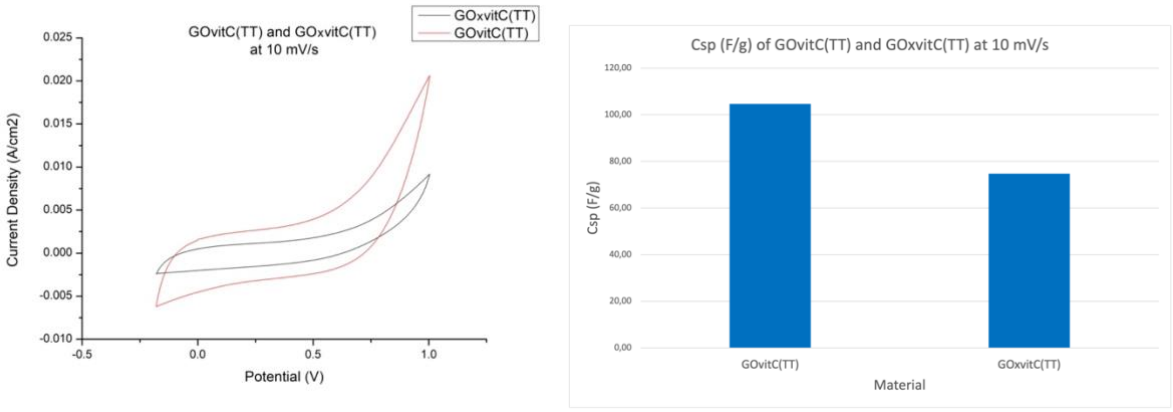


*Figure 16: CV curves and Csp values for GOvitC(TT) and GOxvitC(TT)*

## 3.4 Capacitance study for vitC reduced aerogel, with deposition cycling of Ppy

Previously, it was shown that the GOvitC(TT) sample was the one with the best capacitance, which is the main characteristic we're looking for in our case for energy storage.
So now, it would be interesting to study it in more detail to determine the parameters that could further improve its capacitance. To this end, the sample will still undergo CV electrodeposition, but for 2 different loads. One of 5 cycles and one of 20 cycles.
What we notice is that the 20-cycle electrodeposition has a much steeper curve.

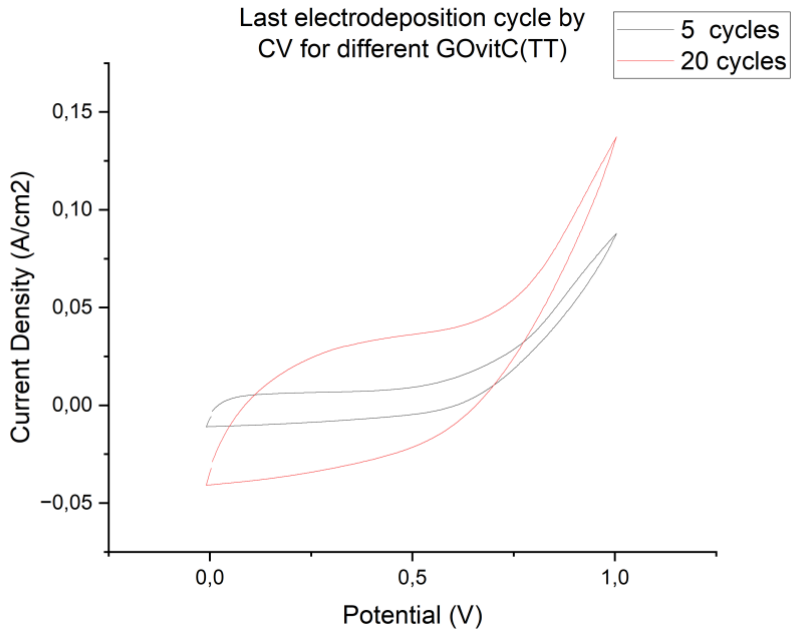


*Figure 17: Electrodeposition of Ppy on different GOvitC(TT) by CV*

Turning now to the curves and Csp values obtained for the different aerogels, we note that all the CV curves are fairly similar, with a larger peak for cvx5. As for Csp values, cvx5 is higher than cvx20. So what we can deduce is that for Ppy electrodeposition on GOvitC(TT) that from 20 cycles, the capacitance values will start to decrease, which is attributed to the tapping of the pores with more Ppy coating, in agreement with previous results.

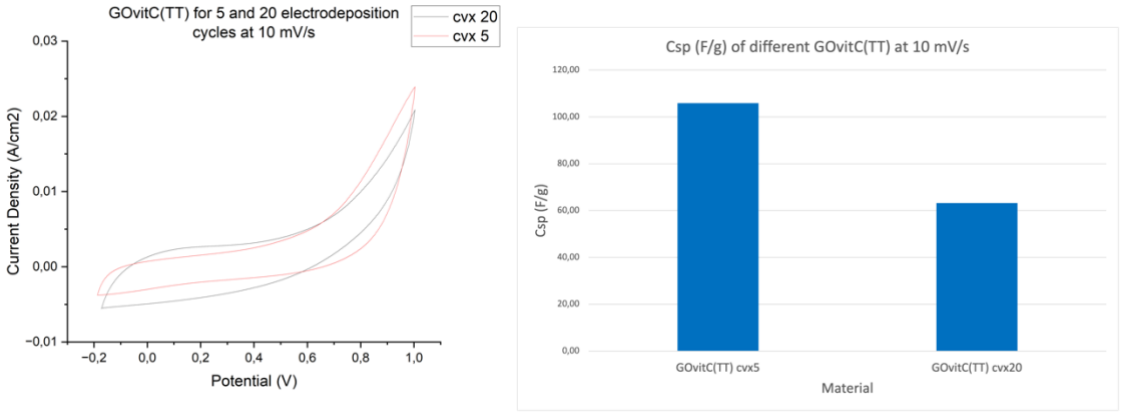


*Figure 18: CV curves and Csp values for different GOvitC(TT)*

Finally, in order to get more precise and more concrete conclusions for improving the capacitance of this aerogel, we need to carry out more experiments with a greater variety in the number of cycles, as well as electroplating with other methods.

# 4 Conclusion

CV electrodeposition of Ppy on different amine-modified graphene oxide aerogels has been carried out, and analysis of the different results helps to understand the differences in specific capacitances between the different samples.

To begin with, from the point of view of aerogel morphology, it should be noted that GO reduction reduces intercalated water molecules and eliminates oxygenated functional groups. The amine groups from EDA and dendrimer G7 improve aerogel pore distribution by reducing pore size, thereby increasing specific surface area. In addition, the amine groups of the dendrimers crosslink with the carboxyl groups of the GO. In addition, CNTs maintain or enlarge the pore size, while vitamin C does not affect pore size but adds stability to the aerogel structure. Finally, after electroplating, Ppy deposition creates a rough surface covered with more or less spherical particles. These fill the pores and form a continuous, homogeneous network with a globular microstructure over the entire surface of the samples.

Next, the specific capacitance values for the different aerogels, which is the main objective of this study, gave interesting values in two cases, for aerogels with and without heat treatment.

Firstly, for aerogels that have not undergone heat treatment. This work shows that the reducing agent EDA provides a better specific capacitance because it distributes better, unlike G7 which, due to its spherical shape, creates non-homogeneous bonds in the aerogel and, during Ppy deposition, hinders the diffusion of electrolyte ions. Moreover, in this case, exfoliation of the GO increases the specific surface area and therefore the specific capacity.

In the case of heat-treated aerogels, the conclusions are different. For both dendrimers, EDA and G7, the specific capacities are lower than for aerogels without dendrimers. This is due to the fact that heat treatment compresses and stuck the sample, which reduces and limits the effective deposition of Ppy and therefore prevents efficient energy storage. This phenomenon is more pronounced in the presence of these reducing agents. It should be noted, however, that G7 and CNT reduce this effect through the spherical shape of the former and the spacer effect of the latter, giving them a better specific capacity than EDA. Moreover, as far as GO(TT) is concerned, its behavior in this case is closer to that of a battery than a supercapacitor.

But above all, this work has shown that the addition of vitamin C to aerogels significantly improves specific capacitance compared with EDA and G7 dendrimers or CNTs. This is simply because vitamin C makes the aerogel more structurally stable, thus limiting the effect of heat treatment, which compresses and stuck the others.
Moreover, in this case, exfoliation is not a good solution. In fact, because of the aerogel's structural stability, it is more conductive, so it will undergo greater Ppy deposition, which will reduce its specific surface area and thus lower its specific capacity compared to an aerogel without vitamin C exfoliation.

# 5 Future work

This study allows us to draw certain conclusions about which reducing agent is most effective in increasing the specific capacitance of the aerogel. Thus, the last part of the study is intended to open the door to future work on vitamin C aerogels. Indeed, the graphs show that the number of cycles during electrodeposition has an influence on specific capacitance. It would therefore be interesting to study the specific capacitance values obtained for different numbers of Ppy electrodeposition cycles for the same material. This would enable us to find the best solution for energy storage. Moreover, there are several electrodeposition methods, and in this study only CV is used. Staying with the same type of aerogel, it therefore seems interesting to study which method achieves the highest value of specific capacitance, i.e. CV, constant potential, constant current.
By carrying out these different analyses on the same aerogel, it may be possible to identify the method and the different parameters that enable us to obtain the material with the best specific capacitance for the desired application.

# 6 Budget

In a project like this, it's really important to take in consideration the cost of the study. To this end, this final section is dedicated to estimating the total project budget. Several categories are taken into account in the calculations.

Firstly, the cost of labor. This cost is estimated by taking into account the work of various people: the project tutor, the laboratory technicians and the student. The details are given in Table 1 below.

| | Cost per hour (€/h) | Number of hours (h) | Cost (€) |
|---|---|---|---|
| Project Tutor | 25 | 60 | 1 500 |
| Laboratory technicians | 17 | 4 | 68 |
| Student | 15 | 300 | 4 500 |
| **Total** | | | **6 068** |

*Table 2: Estimation of labor cost*

Then, of course, there's the depreciation of the machinery, whether SEM, FTIR or the various electrodes. For this, we use the cost of equipment use per hour. This takes into account parameters such as the price of the equipment and its service life. The results are shown in Table 2.

| | Cost per hour (€/h) | Number of hours (h) | Cost (€) |
|---|---|---|---|
| SEM | 30 | 7 | 210 |
| FTIR | 20 | 1 | 20 |
| Oven | 1,8 | 46 | 82,80 |
| Ultrasonic bath | 19 | 2 | 38 |
| Precision balance | 1 | 2 | 2 |
| Pt wire electrode | 0,0095 | 60 | 0,57 |
| Ag/AgCl electrode | 0,0095 | 60 | 0,57 |
| Autolab/PGSTAT101 Metrohm potentiostat | 2 | 60 | 120 |
| **Total** | | | **473,94** |

*Table 3: Depreciation of machinery equipment*

Finally, before and during this work, various materials and tools are used, so their costs need to be taken into account. Estimates are given in Table 3 below. It is important to note that some of the tools shown in Table 3, such as glassware and tweezers, are not disposable and will therefore be reused. This means that the budget for this section is overestimated.

| | Cost per hour (€/quantity) | Quantity | Cost (€) |
|---|---|---|---|
| Graphene oxide | 100€/200mg | 100 mg | 50 |
| EDA | 42,70€/L | 5 mL | 0,21 |
| G7 | 101€/5g | 0,2 mg | 0,01 |
| Vitamin C | 15€/250g | 5 mg | 0,01 |
| CNT | 500€/g | 150 μg | 0,07 |
| PVP | 15€/100g | 150 mg | 0,02 |
| Nitrogen (N2) | 2€/L | 2,85 L | 5,70 |
| Pyrrole | 24€/10mL | 0,34 mL | 0,82 |
| KCl | 35€/25g | 1,86 g | 2,60 |
| $Na_2SO_4$ | 23,70€/25g | 3,55 g | 3,36 |
| Distilled Water | 8€/5L | 2 L | 3,20 |
| Flasks | 28,90€/unit | 2 units | 57,80 |
| Beakers | 10,9€/unit | 4 units | 43,60 |
| Spatula | 4,50€/unit | 1 unit | 4,50 |
| Weighing dishes | 38,20€/500units | 2 units | 0,15 |
| Glass Plates | 2,60€/unit | 39 units | 101,40 |
| Ethanol | 16€/L | 20 mL | 0,32 |
| Scalpel | 168€/100units | 1 unit | 1,68 |
| Tweezers | 7,50€/unit | 1 unit | 7,50 |
| Tape | 3,50€/unit | 0,1 unit | 0,35 |
| Scissors | 2,30€/unit | 1 unit | 2,30 |
| Connecting cables | 12,99€/5units | 3 units | 7,79 |
| Pipette tip | 0,031€/unit | 1 unit | 0,03 |
| **Total** | | | **293,42** |

*Table 4: Cost of materials and tools*

So, after estimating the different aspects of this project, we obtain an estimated total cost of 6 835,36€, as shown in Table 4.

| | Cost (€) |
|---|---|
| Labor | 6 068 |
| Depreciation of machinery equipment | 473,94 |
| Materials and tools | 293,42 |
| **Total** | **6 835,36** |

*Table 5: Total cost for the project*

# References


[1] T.M.I. Mahlia, T.J. Saktisahdan, A. Jannifar, M.H. Hasan, H.S.C. Matseelar, "A review of available methods and development on energy storage; technology update," *Renewable and Sustainable Energy Reviews,* vol. 33, pp. 532-545, 2014. https://doi.org/10.1016/j.rser.2014.01.068

[2] Geoffrey J. May, Alistair Davidson, Boris Monahov, "Lead batteries for utility energy storage: A review," *Journal of Energy Storage,* vol. 15, pp. 145-157, 2018. https://doi.org/10.1016/j.est.2017.11.008

[3] Peter J. Hall, Mojtaba Mirzaeian, S. Isobel Fletcher, Fiona B. Sillars, Anthony J. R. Rennie, Gbolahan. O. Shitta-Bey, Grant Wilson, Andrew Crudenb and Rebecca Carterb, "Energy storage in electrochemical capacitors: designing functional materials to improve performance," *Energy & Environmental Science,* vol. 3, pp. 1238-1251, 2010. https://doi.org/10.1039/C0EE00004C

[4] Lei Zhang, Xiaosong Hu, Zhenpo Wang, Fengchun Sun, David G. Dorrell, "A review of supercapacitor modeling, estimation, and applications: A control/management perspective," *Renewable and Sustainable Energy Reviews,* vol. 81, no. 2, pp. 1868-1878, 2018. https://doi.org/10.1016/j.rser.2017.05.283

[5] Waseem Raza, Faizan Ali, Nadeem Raza, Yiwei Luo, Ki-Hyun Kim, Jianhua Yang, Sandeep Kumar, Andleeb Mehmood, Eilhann E. Kwon, "Recent advancements in supercapacitor technology," *Nano Energy,* vol. 52, pp. 441-473, 2018. https://doi.org/10.1016/j.nanoen.2018.08.013

[6] E. Frackowiak, "Carbon materials for supercapacitor application," *Physical Chemistry Chemical Physics,* vol. 9, pp. 1774-1785, 2007. https://doi.org/10.1039/B618139M

[7] Sahar Yasami, Saeedeh Mazinani, Majid Abdouss, "Developed composites materials for flexible supercapacitors electrode: “Recent progress & future aspects”," *Journal of Energy Storage,* vol. 72, no. E, 2023. https://doi.org/10.1016/j.est.2023.108807

[8] Yu Yang, Yunlong Xi, Junzhi Li, Guodong Wei, N. I. Klyui & Wei Han, "Flexible Supercapacitors Based on Polyaniline Arrays Coated Graphene Aerogel Electrodes," *Nanoscale Research Letters,* vol. 12, no. 394, 2017. https://link.springer.com/article/10.1186/s11671-017-2159-9

[9] Mei Yu, Yuxiao Ma, Jianhua Liu, Songmei Li, "Polyaniline nanocone arrays synthesized on three-dimensional graphene network by electrodeposition for supercapacitor electrodes," *Carbon,* vol. 87, pp. 98-105, 2015. https://doi.org/10.1016/j.carbon.2015.02.017

[10] An Ouyang, Anyuan Cao, Song Hu, Yanhui Li, Ruiqiao Xu, Jinquan Wei, Hongwei Zhu, and Dehai Wu, "Polymer-Coated Graphene Aerogel Beads and Supercapacitor Application," *ACS Applied Materials & Interfaces,* vol. 8, p. 11179–11187, 2017. https://doi.org/10.1021/acsami.6b01965

[11] Lang Ma, Guojian Wang, Jinfeng Dai, "Influence of structure of amines on the properties of amines-modified reduced graphene oxide/polyimide composites," *Journal of Applied Polymer Science,* vol. 133, 2016. https://doi.org/10.1002/app.43820

[12] A.M. Shanmugharaj, J.H. Yoon, W.J. Yang, Sung Hun Ryu, "Synthesis, characterization, and surface wettability properties of amine functionalized graphene oxide films with varying amine chain lengths," *Journal of Colloid and Interface Science,* vol. 401, pp. 148-154, 2013. https://doi.org/10.1016/j.jcis.2013.02.054

[13] Aso Navaee and Abdollah Salimi, "Efficient amine functionalization of graphene oxide through the Bucherer reaction: an extraordinary metal-free electrocatalyst for the oxygen reduction reaction," *RCS Advances,* vol. 5, pp. 59874-59880, 2015. https://doi.org/10.1039/C5RA07892J

[14] Peng Lv, Xun Tang, Ruilin Zheng, Xiaobo Ma, Kehan Yu & Wei Wei , "Graphene/Polyaniline Aerogel with Superelasticity and High Capacitance as Highly Compression-Tolerant Supercapacitor Electrode," *Nanoscale Research Letters,* vol. 12, no. 630, 2017. https://link.springer.com/article/10.1186/s11671-017-2395-z

[15] Joonwon Bae, Jeong Yong Park, Oh Seok Kwon, Chang-Soo Lee, "Energy efficient capacitors based on graphene/conducting polymer hybrids," *Journal of Industrial and Engineering Chemistry,* vol. 51, pp. 1-11, 2017. https://doi.org/10.1016/j.jiec.2017.02.023

[16] Hua Bai, Kaixuan Sheng, Pengfei Zhang, Chun Lia and Gaoquan Shi, "Graphene oxide/conducting polymer composite hydrogels," *Journal of Materials Chemistry,* vol. 11, pp. 18653-18658, 2011. https://doi.org/10.1039/C1JM13918E

[17] Fatemeh Yaghoubidoust, Dedy H.B. Wicaksono, Sheela Chandren, Hadi Nur, "Effect of graphene oxide on the structural and electrochemical behavior of polypyrrole deposited on cotton fabric," *Journal of Molecular Structure,* vol. 1075, pp. 486-493, 2014. https://doi.org/10.1016/j.molstruc.2014.07.025

[18] K. Firoz Babu, S.P. Siva Subramanian, M. Anbu Kulandainathan, "Functionalisation of fabrics with conducting polymer for tuning capacitance and fabrication of supercapacitor," *Carbohydrate Polymers,* vol. 94, pp. 487-495, 2013. https://doi.org/10.1016/j.carbpol.2013.01.021

[19] Wen Tao Yuan, Ya Jie Yang, Yong Long Qiu, Jian Hua Xu, Wen Yao Yang, Shuang Xia, "High Performance Supercapacitor Electrode Materials Based on Activated Carbon and Conducting Polypyrrole," *Key Engineering Materials,* Vols. 645-646, pp. 1150-1155, 2015. https://doi.org/10.4028/www.scientific.net/KEM.645-646.1150

[20] Liyang Yuan, Chuanyun Wan, Liangliang Zhao, "Facial In-situ Synthesis of MnO2/PPy Composite for Supercapacitor," *International Journal of Electrochemical Science,* vol. 10, pp. 9456-9465, 2015. https://doi.org/10.1016/S1452-3981(23)11193-X

[21] Yue Wang, Ruguo Wang, Shichang Xu, Qian Liu & Jixiao Wang, "Polypyrrole/polyaniline composites with enhanced performance for capacitive deionization," *Desalination and Water Treatment ,* vol. 54, pp. 3248-3256, 2015. https://doi.org/10.1080/19443994.2014.907748

[22] Prof. Yibing Xie, Dan Wang, Jingjing Ji, "Preparation and Supercapacitor Performance of Freestanding Polypyrrole/Polyaniline Coaxial Nanoarrays," *Energy Technology,* vol. 4, pp. 714-721, 2016. https://doi.org/10.1002/ente.201500460

[23] Chaoyue Cai, Jialong Fu, Chengyan Zhang, Cheng Wang, Rui Sun, Shufang Guo, Fan Zhang, Mingyan Wang, Yuqing Liucd and Jun Chen, "Highly flexible reduced graphene oxide@polypyrrole–polyethylene glycol foam for supercapacitors," *RSC Advances,* vol. 10, pp. 29090-29099, 2020. https://doi.org/10.1039/D0RA05199C

[24] I. M. Dharmadasa and J. Haigh, "Strengths and Advantages of Electrodeposition as a Semiconductor Growth Technique for Applications in Macroelectronic Devices," *Journal of The Electrochemical Society,* 2005. https://iopscience.iop.org/article/10.1149/1.2128120

[25] E. Roy, "Elaboration Electrochimique et Caractérisations de Nanofils d'Antimoine et d'Or," *HALtheses,* 2002. https://theses.hal.science/tel-00351667

[26] Weilie Zhou, Robert Apkarian, Zhong Lin Wang & David Joy , "Fundamentals of Scanning Electron Microscopy (SEM)," *Scanning Microscopy for Nanotechnology,* pp. 1-40. https://link.springer.com/chapter/10.1007/978-0-387-39620-0_1

[27] K. Vernon-Parry, "Scanning electron microscopy: an introduction," *III-Vs Review,* vol. 13, pp. 40-44, 2000. https://doi.org/10.1016/S0961-1290(00)80006-X

[28] Catherine Berthomieu & Rainer Hienerwadel , "Fourier transform infrared (FTIR) spectroscopy," *Photosynthesis Research,* vol. 101, p. 157–170, 2009. https://link.springer.com/article/10.1007/s11120-009-9439-x

[29] M.A. Mohamed, J. Jaafar, A.F. Ismail, M.H.D. Othman, M.A. Rahman, "Chapter 1 - Fourier Transform Infrared (FTIR) Spectroscopy," *Membrane Characterization,* pp. 3-29, 2017. https://doi.org/10.1016/B978-0-444-63776-5.00001-2

[30] Xiao Xie, Yilong Zhou, Hengchang Bi, Kuibo Yin, Shu Wan & Litao Sun , "Large-range Control of the Microstructures and Properties of Three-dimensional Porous Graphene," *Scientific Reports,* vol. 3, no. 2117, 2013. https://www.nature.com/articles/srep02117

[31] Yan Wang, Yingpeng Wu, Yi Huang, Fan Zhang, Xi Yang, Yanfeng Ma, and Yongsheng Chen, "Preventing Graphene Sheets from Restacking for High-Capacitance Performance," *The Journal of Physical Chemistry C,* vol. 115, no. 46, p. 23192–23197, 2011. https://doi.org/10.1021/jp206444e

[32] "TABLA DE ESPECTRO DE INFRARROJOS POR INTERVALO DE FRECUENCIA," *Merck.* https://www.sigmaaldrich.com/ES/es/technical-documents/technical-article/analytical-chemistry/photometry-and-reflectometry/ir-spectrum-table

[33] "Poly(amidoamine)," *Wikipedia.* https://en.wikipedia.org/wiki/Poly(amidoamine)